

# Modeling the evolution of the Arctic mixed layer during the fall 1997 Surface Heat Budget of the Arctic Ocean (SHEBA) Project using measurements of $^7\text{Be}$

David Kadko

Marine and Atmospheric Chemistry, Rosenstiel School of Marine and Atmospheric Sciences, University of Miami, Miami, Florida

**Abstract.** During the Surface Heat Budget of the Arctic Ocean (SHEBA) project in October 1997 the first measurements of  $^7\text{Be}$  ever made within the Arctic Ocean were used to reconstruct the evolution of the mixed layer over the previous season and confirmed that the reservoir of heat beneath the fall mixed layer was emplaced in the summer, rather than input cumulatively over several seasons or advected in from distant sources. As suggested by *McPhee et al.* [1998], several times as much heat was emplaced at SHEBA than at Arctic Ice Dynamics Joint Experiment 20 years earlier. A likely mechanism for this would be substantially greater lead opening coupled with the positive feedback loop between increased open water, increased heat absorption, and further ice melting. In addition, a rate of net primary production  $\geq 13 \text{ gC m}^{-2}$  for the preceding spring-summer period was derived using this mixed layer history with an oxygen profile from the fall.

## 1. Introduction

One of the important considerations in the summer surface energy balance of the Arctic Ocean is the fate of the energy input (mostly shortwave radiation) in the heterogeneous ice-ocean system during the melt season. Downwelling solar radiation through leads is the primary source for the direct heating of the ocean, but the fate of the solar energy absorbed through the leads is not well understood [*Rind et al.*, 1995]. It is not known for example, the extent to which this heat laterally melts the ice in contact with the leads, is conveyed to depth and melts the ice from below, or is transported away from the ice. The fate of the heat has direct consequence therefore upon the persistence of the ice cover and the associated summertime albedo.

The Surface Heat Budget of the Arctic Ocean (SHEBA) program was undertaken in October 1997 to study the feedbacks associated with the ice-water albedo system, in which the disposition of the summer heat input is of primary importance [e.g., *Ingram et al.*, 1989]. The initial observations made in the Fall of 1997 indicated that the upper ocean was less saline and warmer than expected [*McPhee et al.*, 1998]. The temperature above freezing ( $\delta T$ ) of the mixed layer during SHEBA (1997) had increased by a factor of 2.5 over that which occurred during an earlier program, Arctic Ice Dynamics Joint Experiment (AIDJEX) (1975). Additionally, the mixed layer salinity in 1997 was  $\sim 27.6$  ppt, compared to 29.7 ppt in 1975 [*Maykut and McPhee*, 1995; *McPhee et al.*, 1998]. From this data it was concluded that the oceanic heat flux was considerably greater during the 1997 summer. Because the albedo of open water is considerably less than that of sea ice, it was suggested that the percentage of open water between 1975 and 1997 had tripled to allow a greater amount of heating to occur [*McPhee et al.*, 1998]. It is possible, however, that the heat stored in the

SHEBA mixed layer was the result of cumulative input over several summers or was advected in from elsewhere. Basically, the observations at SHEBA during the fall of 1997 offered only a “snapshot” of the system because no observations were made during the preceding summer. It is therefore difficult to reconstruct the mixed layer evolution and heating history of this site prior to the initial SHEBA occupation.

To address this question, the heat exchange between the leads and underlying mixed layer of the SHEBA site is evaluated here using a naturally occurring radioactive tracer,  $^7\text{Be}$ . Beryllium 7 is a cosmic ray-produced species that is delivered to the Earth’s surface and, as such, is a form of proxy for incoming solar radiation. Because of its 53.3 day half life, it is an ideal tracer of water that has been in contact with the sea surface over the past season [*Kadko and Olson*, 1996]. Profiles of  $^7\text{Be}$  measured in the fall provide an integration of the mixed layer behavior over the previous summer and can offer insight into the mixed layer evolution and heating history.

## 2. Background

Beryllium 7 is a cosmic ray-produced radioactive nuclide with a radioactive mean life of 76.9 days (the mean life is defined as the  $1/e$  decay level or half life/0.693) and, as such, is well suited for studying seasonal phenomenon. Beryllium 7 is deposited upon the Earth’s surface by precipitation and is homogenized within the surface mixed layer of the ocean rapidly with respect to its decay rate [e.g., *Silker*, 1972; *Young and Silker*, 1980; *Kadko and Olson*, 1996]. In snow the  $^7\text{Be}$  activity (equivalent to concentration, here expressed as disintegrations per minute (dpm) per  $\text{m}^3$ ) is  $\sim 2$  orders of magnitude greater than that in the ocean mixed layer because a given  $^7\text{Be}$  flux is diluted in mixed layers typically tens of meters deep but deposited in snow layers (over a 77 day period) that are at least an order of magnitude shallower, thereby concentrating the nuclide relative to the surface ocean [e.g., *Cooper et al.*, 1991]. In the ocean the mixed layer depth is a critical parameter that largely determines the  $^7\text{Be}$  surface activity because for a given

Copyright 2000 by the American Geophysical Union.

Paper number 1999JC900311.  
0148-0227/00/1999JC900311\$09.00

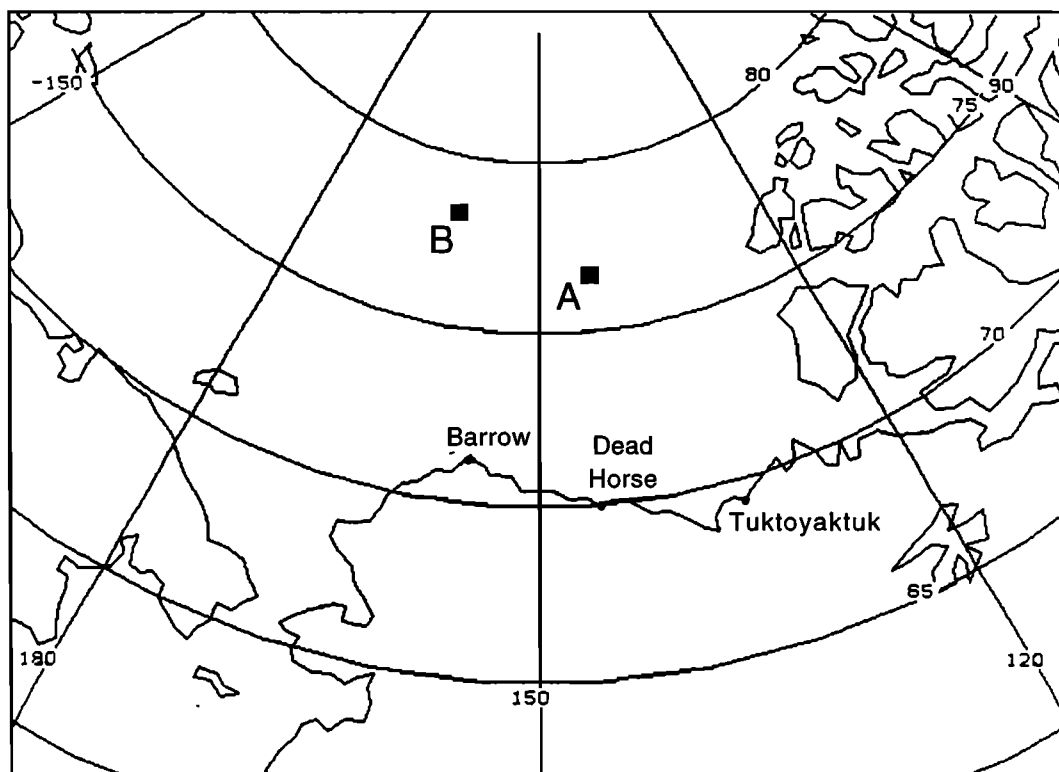


Figure 1. Location map of the Surface Heat Budget of the Arctic Ocean (SHEBA) project site. Point A is the initial deployment location in October 1997. Point B is the location in July 1998.

$^7\text{Be}$  input, the activity is concentrated in shallow mixed layers and diluted in deeper mixed layers. As will be described below, water in contact with the ocean surface is “tagged” with  $^7\text{Be}$ , and profiles of this isotope provide a record of the seasonal changes in the mixed layer depth.

### 3. Methods

Vertical profiles of  $^7\text{Be}$  were collected in the Beaufort Sea from October 8 to 12, 1997 (Figure 1). To collect the samples, a hydrohose was melted through ~2 m of ice through which samples for  $^7\text{Be}$  were collected by pumping. In this process, 700 L of seawater were passed through iron-impregnated acrylic fibers packed in cylindrical cartridges [e.g., *Krishnaswami et al.*, 1972; *Lal et al.*, 1988; *Lee et al.*, 1991; *Kadko and Olson*, 1996]. The water was taken at various depths through a 1.5" hose at the end of which was a conductivity-temperature-depth (CTD) system. The pumping was achieved with a centrifugal pump, powered by a gasoline-fueled generator on the ice, at a rate of ~14 L min<sup>-1</sup>. Thus each sampled depth required ~50 min. In most cases, double or triple samples were collected at any one depth and later combined. On one cast (October 8), where only single cartridges were used at each depth, three samples from different depths in the mixed layer were combined as representative of the mixed layer activity. The fiber efficiency, tested with stable Be in the lab or by counting two cartridges placed in series was  $0.90 \pm .02$ . This is an improvement over earlier fibers [*Kadko and Olson*, 1996] and reflects a higher retention of iron in the fibers produced in the laboratory for this study.

On land the fibers are dried and then ashed. The ash was

placed in a marenelli beaker, which in turn was placed over a low background germanium gamma detector. The  $^7\text{Be}$  has a readily identifiable peak at 478 keV. The detector is calibrated for this geometry by adding a commercially prepared mixed solution of known gamma activities to an ashed fiber and counting it in the marenelli geometry. The counting efficiency for the 478 keV gamma in this configuration was 0.03. The limit of detection used in this work defined at the 99.7% confidence level, is  $S_L = \geq 3\sigma_b$ , where  $\sigma_b$  is the standard deviation of the blank measurements [*Rubinson*, 1987]. The detection limit of a sample increases with time because of  $^7\text{Be}$  decay and, for our system, is  $(12.7/V) \times [\exp(\lambda D)]$  dpm m<sup>-3</sup>, where  $D$  is the number of days after sample collection,  $V$  is the volume (m<sup>3</sup>), and  $\lambda$  is the decay constant (0.013 d<sup>-1</sup>).

To estimate the atmospheric deposition of  $^7\text{Be}$ , samples of snow (m<sup>2</sup> in area) were taken, and also, plastic buckets were deployed to collect fallout over known time periods. The snow was melted, and 0.5 mL of concentrated HCl and stable Be yield tracer were added [e.g., *Dibb*, 1990]. The  $^7\text{Be}$  was removed by coprecipitation with iron hydroxide, dried, and counted by gamma spectrometry. The stable Be in the precipitate was then measured by atomic absorption to calculate the  $^7\text{Be}$  recovery during precipitation. The buckets were deployed for periods ranging between 1 and 3 weeks in October 1997 and July-August 1998. After collection the buckets were rinsed with dilute HCl. Subsequently, the HCl rinse was treated as the snow samples described above and counted [e.g., *Baskaran et al.*, 1993]. The counting system is calibrated for all samples by preparing a commercial standard in geometries identical to the samples.

The error for each measurement is the statistical counting

error  $\sigma$  and the uncertainty in the blank,  $\sqrt{\sigma^2 + \sigma_b^2}$ , multiplied by

$$[(\lambda CT)/[1 - \exp(-\lambda CT)]][\exp(\lambda D)/(CE \cdot FE \cdot PE)],$$

where CT is the counting time, CE is the counting efficiency of the 478 keV gamma, FE is the fiber (or precipitation) efficiency, and PE is the photon emission fraction (0.104) for <sup>7</sup>Be.

#### 4. Results and Discussion

The typical temperature and salinity profile from SHEBA in October 1997 is shown in Figure 2. The mixed layer extended to ~30 m depth, below which was found a layer ~0.5°C warmer than the mixed layer. *McPhee et al.* [1998] note that this layer is appreciably warmer than a similar layer measured during AIDJEX in 1975. The salinity of the mixed layer in SHEBA is also considerably fresher than that of AIDJEX. The <sup>7</sup>Be measurements in October 1997 are presented in Table 1 and displayed with the  $\delta T$  (temperature above freezing) profile in Figure 3a. In two cases the values are close to or below the detection limit defined earlier but are retained because of consistency with the other values (Table 1). The remnant <sup>7</sup>Be below the mixed layer marks the warm water as having been in contact with the sea surface within the previous 77 days. Thus the heated layer beneath the October mixed layer at SHEBA was remnant of an earlier, deeper mixed layer and was the result of very active heat input during the previous late spring-summer. The <sup>7</sup>Be shows that the higher heat layer could not have been advected from afar or emplaced cumulatively over several seasons.

Corresponding to the heat and <sup>7</sup>Be beneath the mixed layer is a peak in oxygen (Figure 3b; profile collected by E. Sherr). The <sup>7</sup>Be gives some insight, at least qualitatively, into the history of this as well. First, it suggests that there had to be substantial primary production early in the melt season when the mixed layer was deep (of the order of 50 m). The presence of substantial open water, a suggested by *McPhee et al.* [1998], would have contributed to sufficient light being available to

**Table 1.** Beryllium 7 From SHEBA, October 1997

Date	Depth, m	<sup>7</sup> Be, dpm m <sup>-3</sup>	Comments
Oct. 8	10, 20, 25	100.8 ± 16.6	three samples combined
Oct. 9	24	103.5 ± 15.0	
	35	24.8 ± 17.7	D.L. <sup>a</sup> = 30.6
Oct. 11	25	133.45 ± 14.0	
	33	30.2 ± 9.2	
	39.6	19.1 ± 6.4	
	45.5	5.95 ± 6.00	D.L. <sup>a</sup> = 12.4
Oct. 12	25	104.7 ± 5.9	
	34	17.8 ± 3.75	
	45	12.5 ± 5.2	

<sup>a</sup>D. L. is the detection limit.

allow phytoplankton activity. Second, while the initial oxygen content is not known and an absolute O<sub>2</sub> utilization rate cannot be determined, the persistence of the oxygen peak well into October suggests that the bacterial respiration rate is low. As discussed below, the data and model presented here allow some estimate of primary production for the summer of 1997 to be determined.

The flux determinations are presented in Table 2. For 1997, if it is assumed that by October 13 snow had been accumulating for 3 weeks at the SHEBA site, then the flux determined by the snow inventory agrees with two out of the three bucket deployments at that time. The average for these measurements is 0.0020 ± 0.0009 dpm cm<sup>-2</sup> d<sup>-1</sup>. In the summer of 1998 the average flux from nine bucket deployments was 0.0122 ± 0.0070 dpm cm<sup>-2</sup> d<sup>-1</sup>.

##### 4.1. Modeling the Mixed Layer Evolution

The distribution of <sup>7</sup>Be can provide quantitative information on mixed layer evolution because features of the <sup>7</sup>Be distribution demand certain aspects of mixed layer history. For example, the presence of <sup>7</sup>Be at a depth of 50 m requires the mixed layer to have been that deep early in the melt season. Furthermore, the mixed layer had to persist long enough at that depth to accumulate sufficient <sup>7</sup>Be to be detected months later in October. In the following the <sup>7</sup>Be is used to derive a mixed layer history that then can be applied to other tracers, notably heat.

The major features of oceanic <sup>7</sup>Be profiles can be generated by accounting for the seasonal deepening and shoaling of the mixed layer on the basis of empirical observations of the mixed layer history. For a given input of <sup>7</sup>Be the mixed layer depth is a critical parameter that largely determines the <sup>7</sup>Be surface activity; shallow mixed layers concentrate <sup>7</sup>Be while in deeper mixed layers the concentration is diluted. The model used here is not dynamically driven, in that there are no surface forcing terms, but simply illustrates how <sup>7</sup>Be (and other surface tracers) will respond to a prescribed mixed layer history, an input function, and relevant tracer decay terms. With this understanding an observed <sup>7</sup>Be profile along with knowledge of <sup>7</sup>Be input can yield insight into the mixed layer history.

Details of the model are presented elsewhere [*Kadko and Olson, 1996*]. It is based on the finite difference form of the one-dimensional analytical expression governing the <sup>7</sup>Be distribution:  $\partial c/\partial t = K_z \partial^2 c/\partial z^2 - \lambda c$ , where  $c$  is the concentration of <sup>7</sup>Be and  $K_z$  is the vertical eddy diffusivity. The <sup>7</sup>Be is assumed to be mixed rapidly with respect to its radioactive decay in the mixed layer and is mixed with a finite  $K_z$  in the pycnocline. As an illustration, the model representation of a

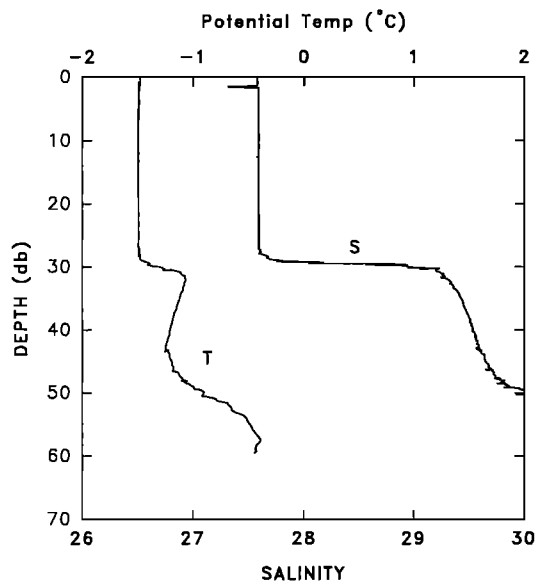


**Figure 2.** Temperature and salinity profiles from October 11, 1997. This profile was typical of those taken between October 8 and 12.

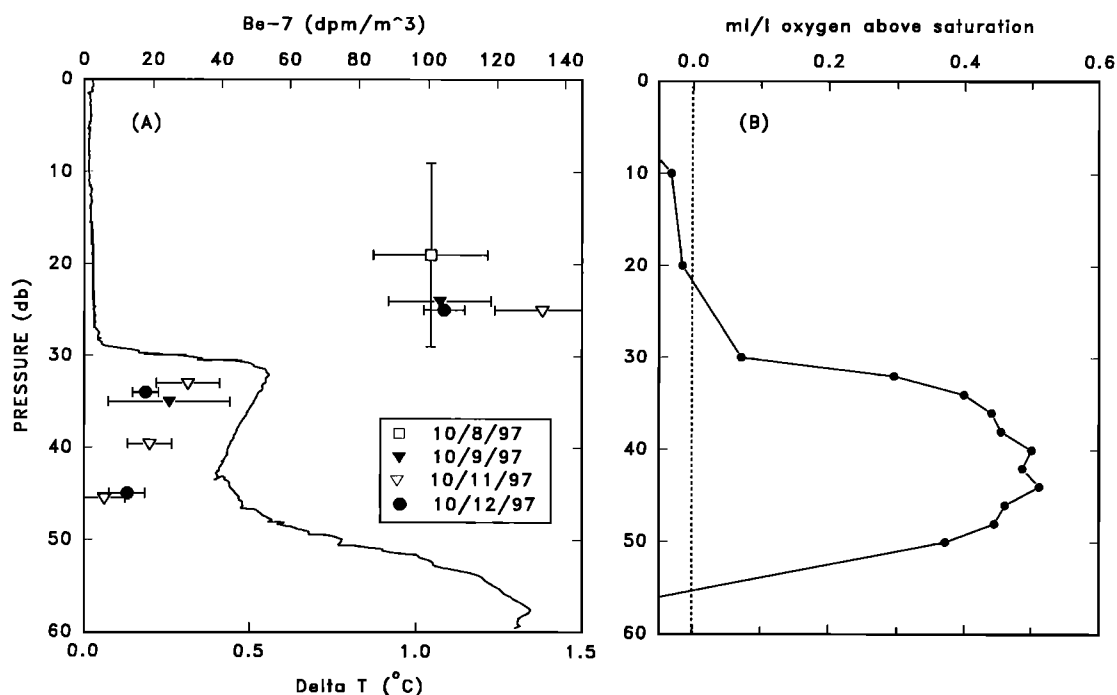


**Figure 3.** (a) The  $^7\text{Be}$  measurements in October 1997 are displayed with the  $\delta T$  profile. The profile is similar to that expected from the model (Figure 4c). (b) The difference ( $\text{O}_2$  concentration minus  $\text{O}_2$  saturation) plotted versus depth for October 24, 1997 (data courtesy of E. Sherr, Oregon State University).

generic seasonal cycle of mixed layer depth is shown in Figure 4a, where at some time ( $T_{\text{max}}$ ) the mixed layer is at its deepest ( $L_{\text{max}}$ ). In this example,  $T_{\text{max}}$  is 50 m, and  $K_z$  for the pycnocline is assigned a value of  $10^{-6} \text{ cm}^2 \text{ s}^{-1}$ .

Monthly profiles of  $^7\text{Be}$  activity are generated as the mixed layer shoals, leaving water beneath the mixed layer that is isolated from the atmospheric input  $I$ , which is chosen to be constant in this example. The  $^7\text{Be}$  activity in the shoaling mixed layer increases, while the  $^7\text{Be}$  isolated at depth decays radioactively, which produces the observed profiles (Figure 4b). In the Arctic, in late Spring and Summer, the mixed layer will

shoal as a result of heat and fresh melt water input until cooling recommences and deepening occurs.

As the mixed layer once again deepens (Figure 4c), the mixed layer  $^7\text{Be}$  concentration decreases because of dilution, and the upper thermocline activity is truncated. This is because the  $^7\text{Be}$  deposited much earlier in the year has now decayed away. This is what was expected at SHEBA in October 1997, at which time the leads and melt ponds were frozen and mixed layer deepening had begun.

In this work the basic model of Kadko and Olson [1996] is modified for the SHEBA site. The parameters used for the

**Table 2.** Flux Measurements

Sample	Collection Dates	Collection Time, days	Flux, $\text{dpm cm}^{-2} \text{ d}^{-1}$
Bucket 1	Oct. 2–10, 1997	7.9	0.0020
Bucket 2	Oct. 3–15, 1997	11.8	0.0005
Bucket 3	Oct. 4–15, 1997	10.9	0.0021
Snow 1	Oct. 13, 1997	21 <sup>a</sup>	0.0031
Snow 2	Oct. 13, 1997	21 <sup>a</sup>	0.0022
Average Oct. 1997			$0.0020 \pm 0.0009$
Bucket 4	July 5–20, 1998	15.2	0.0092
Bucket 6	July 5–20, 1998	15	0.0028
Bucket 7	July 6–20, 1998	14	0.0058
Bucket 8	July 12–29, 1998	17	0.0233
Bucket 9	July 20 to Aug. 8, 1998	17	0.0192
Bucket 10	July 20 to Aug. 8, 1998	17	0.0177
Bucket 11	July 20 to Aug. 8, 1998	17	0.0127
Bucket 12	July 21 to Aug. 10, 1998	20.1	0.0143
Bucket 13	July 30 to Aug. 10, 1998	10.75	0.0052
Average July–August 1998			$0.0122 \pm 0.0070$

<sup>a</sup>Assumed snow accumulation time.

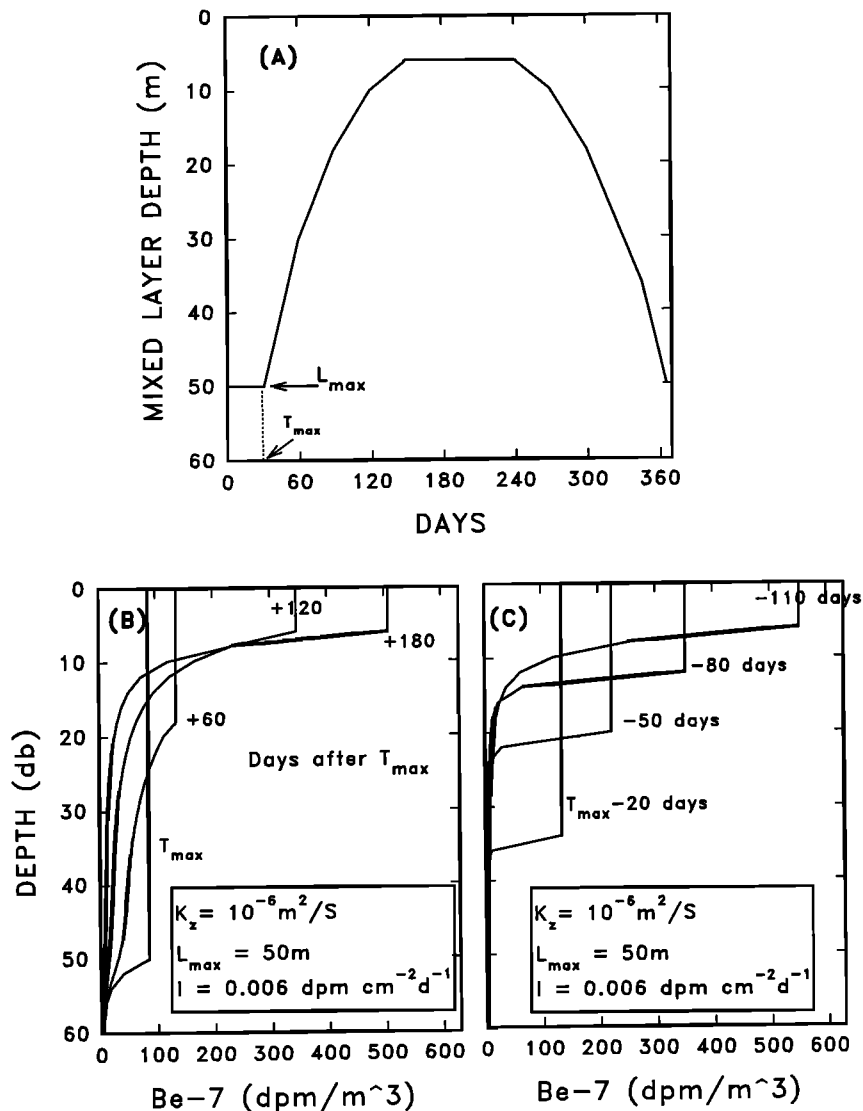


**Figure 4.** (a) The model representation of an idealized seasonal cycle of mixed layer depth where at some time ( $T_{max}$ ) the mixed layer is at its deepest ( $L_{max}$ ). In this example the input of  $^7\text{Be}$ ,  $I$ , is constant over the entire seasonal cycle, and  $K_z$  in the pycnocline is chosen to be  $10^{-6} \text{ m}^2 \text{ s}^{-1}$ . (b) The  $^7\text{Be}$  activity for a shoaling mixed layer. Profiles of  $^7\text{Be}$  are generated for various times (+ days after  $T_{max}$ ). As shoaling progresses, the  $^7\text{Be}$  activity of the mixed layer increases, while the  $^7\text{Be}$  isolated at depth decays radioactively, which produces the observed tailing. (c) As the mixed layer once again deepens, the mixed layer  $^7\text{Be}$  concentration decreases because of dilution and the upper thermocline activity is truncated. This is because the  $^7\text{Be}$  deposited much earlier in the year has now decayed away. Profiles that might be expected at SHEBA in the fall during mixed layer deepening would be similar to these model curves.

1997 summer-fall in SHEBA are displayed in Figure 5, and the model output is shown in Figure 6. Monthly profiles of  $^7\text{Be}$  are derived as a function of mixed layer evolution and  $^7\text{Be}$  input. Initially, it is assumed that there is no  $^7\text{Be}$  in the ocean following the winter when the ice-covered upper ocean had been isolated from atmospheric input.

The input function here is somewhat different than that of Kadko and Olson [1996] in that input of  $^7\text{Be}$  is not constant. Here it is comprised not only of atmospheric input but additionally, during late spring, of rapid input from melting snow that has accumulated  $^7\text{Be}$  over the winter months. The  $^7\text{Be}$  input function consisted of three stages (Figure 5). In stage 1, from June 21 (summer solstice) until July 19,  $^7\text{Be}$  was input through atmospheric flux and snow melt. In stage 2, from July

19 to September 20, there is only atmospheric input. In stage 3, there is zero  $^7\text{Be}$  input because of ice cover. The model is run until October 11, at which time the SHEBA site was completely frozen and snow covered, i.e., isolated from atmospheric or melt input. Likely, it had been in this state of the order of 3 weeks. Therefore, from September 20 to October 11, there is zero  $^7\text{Be}$  input (i.e., there is only  $^7\text{Be}$  decay).

The atmospheric flux is determined as follows: on October 11 the depth-integrated standing stock of  $^7\text{Be}$  was  $0.357 \text{ dpm cm}^{-2}$ . Correcting this to September 20, the standing stock of  $^7\text{Be}$  before isolation would be  $0.463 \text{ dpm cm}^{-2}$ , corresponding to flux of  $0.463\lambda$  or  $0.006 \text{ dpm cm}^{-2} \text{ d}^{-1}$ , which is the input used between July 19 and September 20 (stage 2). It is then assumed that the atmospheric flux accumulating in the snow

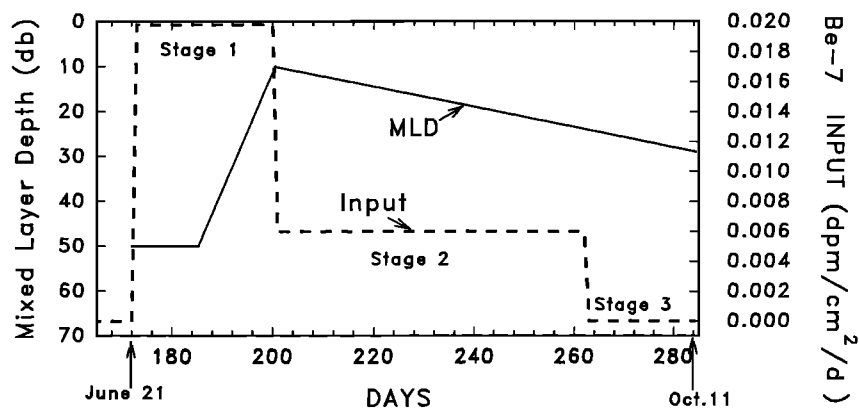


Figure 5. Parameters used in the SHEBA  $^7\text{Be}$  model as a function of time. The three stages of  $^7\text{Be}$  input are shown.

during the winter months was the same as during the stage 2 flux, and thus the standing stock of  $^7\text{Be}$  in the snow would be  $0.463 \text{ dpm cm}^{-2}$ . Assuming snow melt occurred predominately over a month's time, this  $^7\text{Be}$  is input into the water gradually over the 28 day period of stage 1. The formulation for stage 1 is

$$\begin{aligned} \text{Input}_{\text{total}} &= \text{Input}_{\text{melt}} + \text{Input}_{\text{atm}} \\ &= \{(0.463/28)[1 - \exp(-(\lambda 28))]/(\lambda 28)\} \\ &\quad + 0.006 \text{ dpm cm}^{-2} \text{ d}^{-1}. \end{aligned}$$

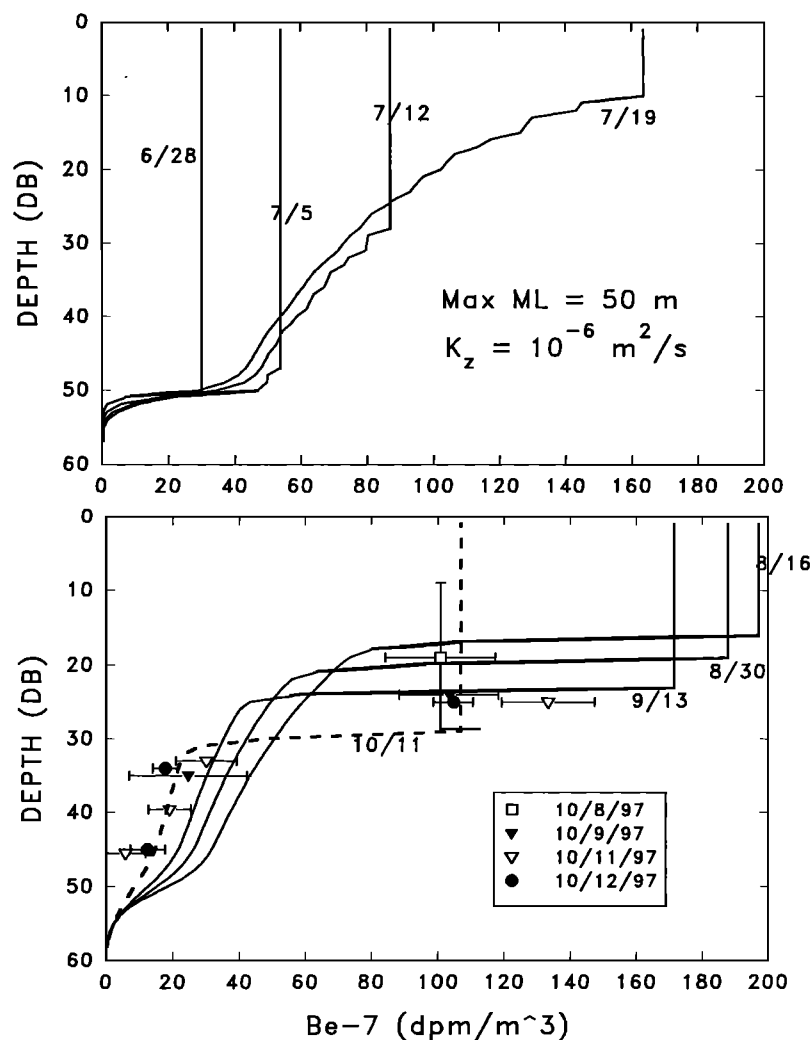
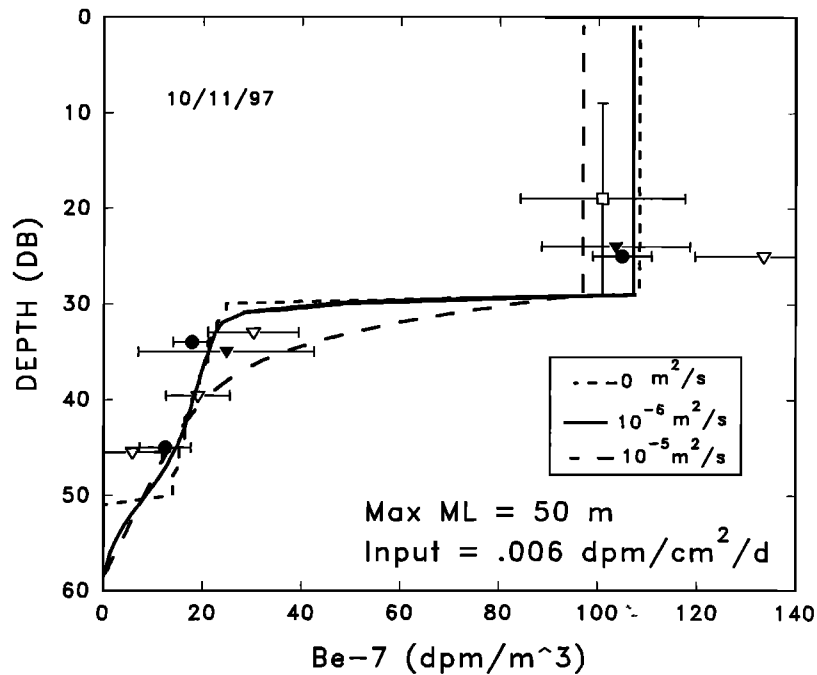


Figure 6. The model output showing the evolution of the  $^7\text{Be}$  profile at SHEBA with time. Data from the period October 8–12 are superimposed upon the model profiles. The model profile for October 11 is shown as a dashed line.



**Figure 7.** The model output for the  $^7\text{Be}$  profile at October 11 for three different values of  $K_z$  in the pycnocline: 0,  $10^{-6}$ , and  $10^{-5} \text{ m}^2 \text{ s}^{-1}$ .

From the maximum depth of the  $^7\text{Be}$  it is surmised that at the onset of melting the maximum depth of the mixed layer was 50 m. This assumes that mechanisms such as downwelling were not a factor, which is reasonable as the SHEBA site was not in the center of an anticyclonic gyre. Starting June 21 (summer solstice) this depth is maintained for 12 days following which the mixed layer decreases to a minimum of 10 m on July 19. With the  $^7\text{Be}$  input flux used a late spring mixed layer maintained at this depth for this time period is required to achieve the  $^7\text{Be}$  profile observed in October. The maximum mixed layer depth modeled here is similar to that reported for the Canadian Basin at ice island T-3 from 1970 to 1973 [Morison and Smith, 1981] and for the AIDJEX project in 1975 [Maykut and McPhee, 1995].

The effect of different pycnocline  $K_z$  on the model results is shown in Figure 7. These results suggest that in the highly stratified water below the mixed layer (see salinity gradient in Figure 2), vertical mixing is not much greater than  $10^{-6} \text{ cm}^2 \text{ s}^{-1}$  and that the  $^7\text{Be}$  profile is mainly a response to the fall deepening of the mixed layer. Higher values of  $K_z$  would draw more  $^7\text{Be}$  from the mixed layer into the pycnocline water.

The flux used in the model ( $0.006 \text{ dpm cm}^{-2} \text{ d}^{-1}$ ) lies between the flux determinations of October 1997 ( $0.0020 \text{ dpm cm}^{-2} \text{ d}^{-1}$ ) and July-August 1998 ( $0.0122 \text{ dpm cm}^{-2} \text{ d}^{-1}$ ). As such, the model value is not unreasonable, but there is no historical  $^7\text{Be}$  flux data from this area of the world with which to compare it. Taken at face value, the ratio of the model flux (based on the summer 1997 water inventory) to the measured summer 1998 flux ( $\sim 0.5$ ) could suggest that in 1997 the summertime lead coverage was of the order of 50%. This appears large and is certainly biased by  $^7\text{Be}$  input from meltwater runoff. However, the large heat inventory measured in October 1997 suggests that indeed, substantial open water must have been present. This will be discussed in section 4.2.

#### 4.2. Modeling the Evolution of Mixed Layer Temperature

The evolution of the  $^7\text{Be}$  distribution in the model described above is similar to the evolution of  $\delta T$  described by Maykut and McPhee [1995]. In late winter, there is a deep, well-mixed layer. After 2 months, spanning the summer solstice, there is warming throughout the mixed layer and freshening due to melt water introduced at the surface. By late summer the mixed layer has shoaled, leaving deeper water behind that had been heated earlier in the season. The maximum in  $\delta T$  is interpreted to be the temperature to which the mixed layer was heated around the time of the solstice and, like the deep  $^7\text{Be}$  is a remnant feature of the deeper mixed layer of late spring/early summer. In a sense this is a form of subduction in which water, initially in contact with the surface, becomes isolated from the atmosphere. The heat is trapped in this layer until subsequent wintertime convection.

In the modeling shown below the temperature maximum is similarly formed, i.e., as a consequence of meltwater capping and represents a residual mixed layer. However, it is shown that the  $\delta T$  maximum likely corresponds to the temperature to which the mixed layer was heated by mid-July (as opposed to the solstice) and marks the depth of the mixed layer at that time.

The parameters used in the temperature evolution model are shown in Figure 8. The model is the same as that used for  $^7\text{Be}$  except that there is no radioactive decay term and it uses the mixed layer evolution derived from the  $^7\text{Be}$  distribution (compare Figures 5 and 8). The heat input function was derived from the pattern of summer heat content of the water column during AIDJEX in 1975 (Figure 9 [from Maykut and McPhee, 1995, Figure 9]). At AIDJEX (Snowbird site), starting approximately June 21, the heat content increased at a rate of  $9.64 \text{ W m}^{-2}$  for a period of 28 days (Figure 8, line a). For the next 39 days the net heat increase was at a rate of  $0.48 \text{ W m}^{-2}$

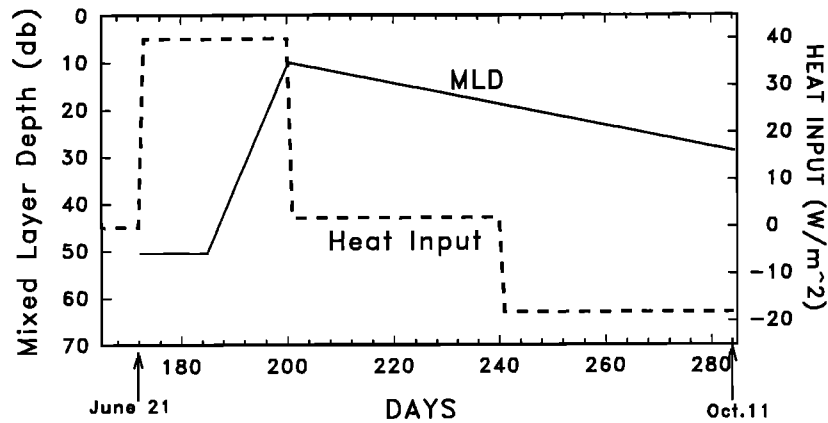


**Figure 8.** The parameters used in the temperature evolution model plotted as a function of time. The model uses the mixed layer evolution derived from the  $^7\text{Be}$  distribution.

(Figure 8, line b). Beyond that date, there was a net heat loss of  $-4.4 \text{ W m}^{-2}$  (Figure 8, line c). To achieve the temperature profile observed on October 11, 1997, with this model, the same relative heat flux for each period was used, but the absolute values had to be quadrupled (39, 2, and  $-18 \text{ W m}^{-2}$ , respectively). This is consistent with *McPhee et al.* [1998], who suggest that the lead openings in 1997 relative to AIDJEX (1975) tripled, and with observations made at SHEBA in October that indicated extensive summertime melting. These included thinner ice than anticipated ( $\sim 1.2 \text{ m}$  as opposed to 3–4 meters), extensive melt pond (by then frozen) coverage, and melt ponds that had melted through to the underlying ocean (D. Perovich, personal communication, 1998). This is also consistent with the high  $^7\text{Be}$  inventory (relative to flux) of the water column measured in October 1997, which requires substantial lead opening for the  $^7\text{Be}$  to enter the upper ocean.

The model output is shown in Figure 10 comparing the case of AIDJEX and SHEBA. It is seen that the  $\delta T$  maximum on October 11 corresponds to the temperature to which the mixed layer was heated by mid-July and marks the depth of the mixed layer at that time. These results are consistent with the conclusion drawn by *McPhee et al.* [1998] that the mixed layer was of the order of 50 m deep early in the summer, was extensively heated before shoaling, and by October had given up its available heat. By using  $^7\text{Be}$ , similar conclusions are independently drawn.

#### 4.3. Modeling the Evolution of Mixed Layer Oxygen and Implications for Primary Production

By analogy with the temperature profile the peak in oxygen measured in October 1997 is remnant of spring-summer production, while the water above it has subsequently degassed during mixed layer deepening. Neglecting for the moment loss effects through respiration, the upper 50 or so meters must have been at least  $0.5 \text{ mL L}^{-1}$  or  $35 \text{ g m}^{-2}$  above saturation. This is of the order of  $13 \text{ gC m}^{-2}$  net production but likely represents a minimum because (1) if this production commenced in June, then the water column started out below saturation as a result of respiration during the dark season, (2)  $\text{O}_2$  is lost through gas exchange, and (3) respiration occurred subsequent to the summer. The 1998 spring-summer observations at SHEBA are consistent with this estimate. Although direct comparison may not be possible because the SHEBA site had drifted far west from the October 1997 location (Figure 2), the June-July net production of oxygen suggested a net community primary production of  $\sim 17 \text{ gC m}^{-2}$  (B. Sherr, personal communication, 1998).

#### 5. Conclusions

This paper reports the first measurements of  $^7\text{Be}$  ever made within the Arctic Ocean. The profile from October 1997 was used to reconstruct the evolution of the mixed layer over the

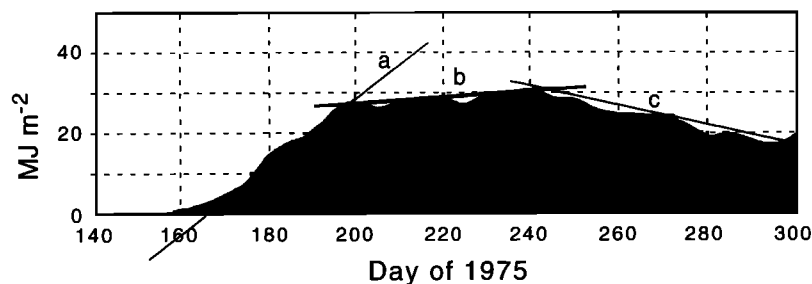


**Figure 9.** The pattern of summer heat content of the water column during Arctic Ice Dynamics Joint Experiment (AIDJEX) in 1975 [from *Maykut and MCPhee*, 1995]. The heat input for SHEBA (1997) was derived by quadrupling the slope of the three lines pictured here.

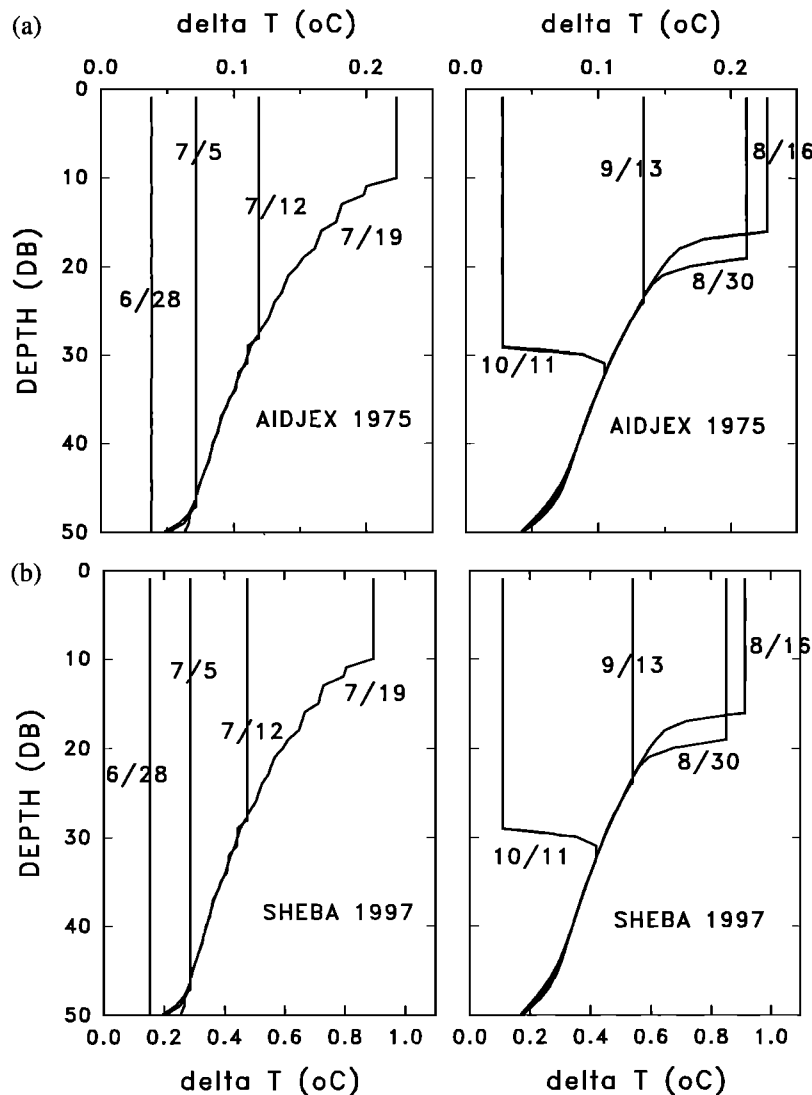


**Figure 10.** The model temperature output for (a) AIDJEX and (b) SHEBA. Note the change in temperature scale. It is seen that the  $\delta T$  maximum on October 11 corresponds to the temperature to which the mixed layer was heated by mid-July (as opposed to the solstice) and marks the depth of the mixed layer at that time.

previous season and confirmed that the reservoir of heat beneath the fall mixed layer was emplaced in the summer, rather than input cumulatively over several seasons or advected in from distant sources. In addition, a reasonable rate of primary production for the spring-summer period was derived using this mixed layer history with an oxygen profile from the fall.

As suggested by *McPhee et al.* [1998], several times as much heat was emplaced at SHEBA than at AIDJEX 20 years earlier. A likely mechanism for this is substantially greater lead opening coupled with the positive feedback loop between increased open water, increased heat absorption, and further ice melting. Note that while the heat observed in October was not cumulative (i.e., the heat is reset each winter), a portion of the salinity change can be cumulative. Consistent with observations of accelerating diminishment of Arctic sea ice [*Johannessen et al.*, 1995], the change in salinity might be an ongoing process that has been occurring over many summers of increased oceanic heat absorption.

**Acknowledgments.** This work was supported by NSF Polar Program (grant OPP-9701067) and by the NSF Chemical Oceanography Program (grant OCE-9809168). The author would like to thank J. Morison, M. McPhee, and B. Welch for many valuable discussions in regards to this paper and two anonymous reviewers for their helpful comments. Thanks also to E. Sherr and B. Sherr for permission to present their oxygen data and to M. Stephens for field and laboratory assistance. Finally, the author acknowledges the crew of the CCGC DES Groseilliers and the SHEBA logistics group for their support during the field operation of SHEBA.

## References

- Baskaran, M., C. H. Coleman, and P. H. Santchi, Atmospheric depositional fluxes of  $^7\text{Be}$  and  $^{210}\text{Pb}$  at Galveston and College Station, Texas, *J. Geophys. Res.*, 98, 20, 555–20, 571, 1993.
- Cooper, L. W., C. R. Olsen, D. K. Solomon, I. L. Larsen, R. B. Cook and J. M. Grebmeier, Stable isotopes of oxygen and natural and fallout radionuclides used for tracing runoff during snowmelt in an Arctic watershed, *Water Resour. Res.*, 27, 2171–2179, 1991.
- Dibb, J. E., Beryllium-7 and lead-210 in the atmosphere and surface

- snow over the Greenland ice sheet in the summer of 1989, *J. Geophys. Res.*, *95*, 22, 407–22, 415, 1990.
- Ingram, W. J., C. A. Wilson, and J. F. B. Mitchell, Modeling climate change: An assessment of sea ice and surface albedo feedbacks, *J. Geophys. Res.*, *94*, 8609–8622, 1989.
- Johannessen, O. M., M. Martin, and E. Bjørgo, The Arctic's shrinking sea ice, *Nature*, *376*, 126–127, 1995.
- Kadko, D., and D. Olson, Be-7 as a tracer of surface water subduction and mixed layer history, *Deep Sea Res., Part II*, *43*, 89–116, 1996.
- Krishnaswami, S., D. Lal, B. L. K. Somayajulu, F. S. Dixon, S. A. Stonecipher, and H. Craig, Silicon, radium, thorium and lead in seawater; In-situ extraction by synthetic fibre, *Earth Planet Sci. Lett.*, *16*, 84–90, 1972.
- Lal, D., Y. Chung, T. Platt and T. Lee, Twin cosmogenic radiotracer studies of phosphorus recycling and chemical fluxes in the upper ocean, *Limnol. Oceanogr.*, *33*, 1559–1567, 1988.
- Lee, T., E. Barg and D. Lal, Studies of vertical mixing in the Southern California Bight with cosmogenic radionuclides  $^{32}\text{P}$  and  $^7\text{Be}$ , *Limnol. Oceanogr.*, *36*, 1044–1053, 1991.
- Maykut, G. A., and M. G. McPhee, Solar heating of the Arctic mixed layer, *J. Geophys. Res.*, *100*, 24, 691–24, 703, 1995.
- McPhee, M. G., T. P. Stanton, J. H. Morison and D. G. Martinson, Freshening of the upper ocean in the central Arctic: Is perennial sea ice melting?, *Geophys. Res. Lett.*, *25*, 1729–1732, 1998.
- Morison, J. H., and J. D. Smith, Seasonal variations in the upper Arctic as observed at T-3, *Geophys. Res. Lett.*, *8*, 753–756, 1981.
- Rind, D., R. Healy, C. Parkinson, and D. Martinson, The role of sea-ice in 2 x CO<sub>2</sub> climate model sensitivity, Part 1, The total influence of sea ice thickness and extent., *J. Clim.*, *8*, 449–463, 1995.
- Rubinson, K. A., *Chemical Analysis*, Little, Brown, Boston, Mass., 1987.
- Silker, W. B., Beryllium-7 and fission products in the GEOSECS II water column and applications of their oceanic distributions, *Earth Planet. Sci. Lett.*, *16*, 131–137, 1972.
- Young, J. A., and W. B. Silker, Aerosol deposition velocities on the Pacific and Atlantic Oceans calculated from  $^7\text{Be}$  measurements, *Earth Planet. Sci. Lett.*, *50*, 92–104, 1980.

---

D. Kadko, RSMAS/MAC, University of Miami, 4600 Rickenbacker Causeway, Miami, FL 33149. (dkadko@rsmas.miami.edu)

(Received January 23, 1999; revised September 10, 1999; accepted October 6, 1999.)